

Kinetic Studies on the Tensile State of Water in Trees

Helmut Tributsch,^{*,†} Jan Cermak,[‡] and Nadezhda Nadezhkina[‡]

Department Solare Energetik, Hahn-Meitner Institute, 14109 Berlin, Germany, and Institute of Forest Ecology, Mendel University, Zemedelska 3, 613 00 Brno, Czech Republic

Received: March 10, 2005; In Final Form: June 15, 2005

The solar-powered generation and turnover of tensile, cohesive water in trees is described as a kinetic phenomenon of irreversible thermodynamics. A molecular kinetic model for tensile water formation and turnover is presented, which is found to be mathematically equivalent with an autocatalytic reaction (Brusselator). It is also shown to be consistent with the van der Waals equation for real liquid–gas systems, which empirically considers intermolecular forces. It can therefore be used to explain both the irreversible thermodynamics and the kinetics of the tensile liquid state of water. A nonlinear bistable evaporation behavior of tensile water is predicted, which has not yet been experimentally characterized in trees. Conventional sap flow techniques in combination with infrared imaging of heat flow around a local heat source were used to study the dynamics and energetics of water transport of trees during the eclipse of August 11, 1999. The evaporative “pulling force” in a tree was demonstrated with infrared techniques and shown to respond within seconds. While the ambient temperature during the eclipse did not drop by more than 2 °C, evaporative water transport was reduced by a factor of up to 2–3. The expected hysteresis (with an up to 50% decrease in energy-conversion-related entropy production) was measured, reflecting a bistable mode of conversion of solar energy into tensile water flow. This nonlinear (autocatalytic) phenomenon, together with tensile molecular order, damped the oscillating behavior of xylem tensile water, and its occasional all-or-none rupture (cavitation) can thus be explained by the nonlinear nature of intermolecular forces active in the water conduit/parenchyma environment. This characterizes the physical chemistry and energetics of tensile water in trees as an active-solar-energy-driven self-organizing process. Water is handled in the form of microcanonical ensembles and transformed into a stretched, metastable icelike state with stronger hydrogen bonding and increased heat of evaporation. The discussed model may open new opportunities for research and understanding toward innovative water technologies.

Introduction

Solar energy conversion via evaporation of capillary water from plants for the purpose of lifting and distributing water, of evaporative cooling, or of desalination (mangroves) turns over much more solar energy than photosynthesis. During this process, water is lifted under tension 100 m high or sucked from a water-deficient or saline underground with intermolecular hydrogen and van der Waals bonding sustaining molecular cohesion. Many physical chemical and physiological aspects of this phenomenon have been investigated and discussed.^{1–11} Complicated phenomenological model calculations have been performed.¹² Implications such as forest decline due to pollution have also been linked to tensile water properties.¹³ But, beyond experimental demonstration of tensile strength in water, it has not yet been possible to reproduce and handle tensile water systems technologically.¹⁰ One reason is the difficulty to sustain tensile strength in water for a reasonably long time, without risking cavitation, which is suppressed in tree capillaries, where typically “negative” pressures of 0.5–3 MPa or 5–30 bar are observed at noon. The strength limits of tensile water have been estimated to reach 10% of that produced by metallic copper or aluminum. Practically no research has been done on the

mechanism of coupling of solar radiation with tensile water evaporation within the leaves of trees so that the concept exists that conventional evaporation processes as known from technical thermodynamics for nontensile water prevail. This implies that water vapor in the leaf structure is in equilibrium with sap water and that tensile water in the plant water conduits is just generated as a side product of evaporation, which turns over substantial energy. The fact that despite nature’s amazing examples of tensile water technology no artificial systems could be established during the last century of fast scientific progress shows that a gap in fundamental understanding of the physical chemistry of tensile water exists. While it is well-established that stronger bonded “vicinal” water exists in nano- and microstructured environments, it has not been studied how it could be handled for bio-similar technical applications. This will be done in this contribution, which additionally investigates to what extent the assumptions of equilibrium thermodynamics are justified for water subject to cohesion–tension dynamics. Because it is found that the constraints of reversible thermodynamics are in contradiction, it is attempted to understand the molecular kinetics of tensile water turnover within the frame of irreversible thermodynamics.

Water is of course an extremely well-studied medium, which has nevertheless remained attractive for modern research. It is well-known that hydrogen bonds play a significant role in sustaining the intermolecular attraction and that more of these hydrogen bonds are active in ice, where bond distances are

* Author to whom correspondence should be addressed. Phone: +49 30 80 62 2247. Fax: +49 30 80 62 2434. E-mail: tributsch@hmi.de.

[†] Hahn Meitner Institute.

[‡] Mendel University.

known to be larger than in water (various structures of ice exist). Stretching the structure of water, where only a smaller portion of water molecules are clustered via hydrogen bonds, may thus enable a larger concentration of hydrogen bonds to be active. The tensile state of water may be a state, to some extent approaching the expanded structure of ice, in which more hydrogen bonds are activated as compared to the normal state of water.

Materials and Methods

Experimental Strategy. The idea of this work was to monitor sap movements and correlated evaporation in trees by introducing heated needles into living tree trunks and to monitor sap flow via thermal sensors and infrared imaging. To avoid artificial environmental influences on the tree that could have affected evaporation of water, advantage was taken of the August 11, 1999, solar eclipse at noon to study the effect of solar energy shading on the kinetics of evaporation. The results were intended for testing of a new theoretical model on tensile state water.

Site and Sample Trees. Experiments were performed in sample trees situated in the park of the Hahn Meitner Institute in Berlin, Germany, during August 1999. Two lime sample trees (*Tilia cordata* Mill.) with similar diameters at breast height (Tilia_1, 15.3 cm and Tilia_2, 14.8 cm) were selected for the study.

The first sample tree, Tilia_1, was prepared for taking frontal images of the heat field around the heater (a heated needle) during the eclipse of August 11, 1999. This was achieved by cutting off the outer segment of the stem (20 cm long) down to the depth of 2.6 cm from the northern stem side (Figure 1, top panel). The xylem surface (which carries the water-conducting channels) opened this way was then smoothed by a sharp knife, and the IR camera was focused on the smooth surface. The multipoint heat field deformation (HFD) sap flow sensor was installed from the opposite (southern) side of stem, so that the tip of the long heater reached the smooth surface. The heated point visible on the smoothed stem surface occurred at a depth corresponding to the middle sapwood approximately. The heat field generated by the linear heater (heated hypodermic needle) was then simultaneously recorded by the series of multipoint thermometers and by the IR camera, which visualized its frontal image.

The second sample tree, Tilia_2, was prepared to obtain the radial image of the heat field around the heater (Figure 1, right panel) during the severing experiment to observe the evaporation pulling force. A larger part of the stem was cut off (down to the depth of 4.5 cm from the eastern side of the stem), and its surface was smoothed as in the previous case. The same radial sap flow sensor was installed in the stem, but in parallel to the smooth stem surface, so that a heat profile across the stem could be generated, which showed the effect of water flow in the two xylem regions facing the bark of the tree. This way, it was made possible to monitor the radial (parallel to the stem radius) IR images of the heat field periodically and to obtain a continuous record of sap flow at the same time. For the demonstration of pulling force, the stem was cut down to the pith 20 cm above the sensor from one of its sides.

Trees during the eclipse were studied also simultaneously in the Czech Republic near Brno (Sobesice forest) exposed to a 90–95% solar eclipse. Sap flow was measured by the HFD method at two heights of a maple tree (diameter at breast height (DBH) equal to 27.5 cm) at breast height and at height of 11 m just below the crown of the main branch. Another sample tree

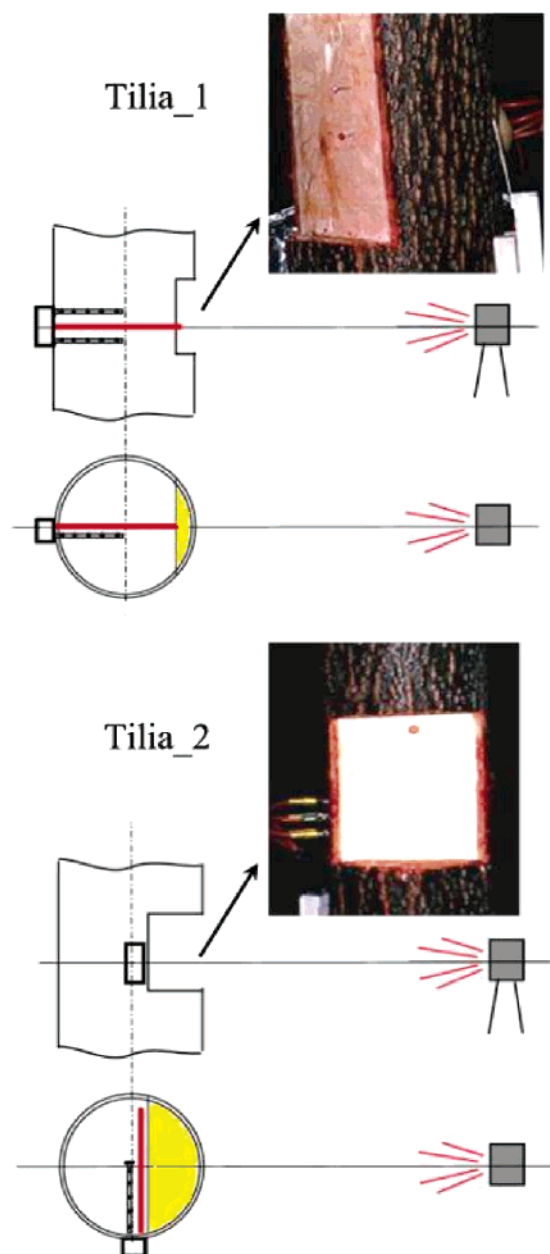


Figure 1. Preparation of lime trees for sap flow measurements by the heat field deformation (HFD) sensor and an infrared imaging heat field generated by the linear heater (marked by the red line) inserted in tree stems. Tilia_1 was prepared for frontal imaging of the heat field (top panel) during the eclipse, whereas Tilia_2 was prepared for the radial view of the heat field (bottom panel) during severing treatment when half of the stem was cut down to pith 20 cm above the HFD sensor. Shaded areas in both stem cross sections correspond to cut-off parts of stems.

was lime (DBH equal to 27 cm), and measurements of sap flow were also carried out at two heights at DBH and a height of 12.6 m.

Meteorological data on solar light intensity, temperature, humidity, and wind velocity were collected close to the experimentation sites.

Sap Flow Measurements. Sap flow was measured by the HFD method.^{13–15} A small region within the water-conducting xylem structure of the tree is heated, and the heat field pattern changes due to the variable tree sap flow monitored. Sensors consisted of a long linear heater and two pairs of thermocouples, one of which was placed symmetrically up and down from the heater (measured symmetrical temperature difference dT_{sym}),

while the other was placed asymmetrically on one side of the heater (measured asymmetrical temperature difference dT_{as}). The heater and the thermocouples were mounted in stainless steel hypodermic needles (six pairs of the thermocouples per needle were applied for sap flow measurements in different sapwood depths along the xylem radius). The ratio of both measured temperature gradients (dT_{sym}/dT_{as}), the geometry of the measuring point, and appropriate physical constants were applied for calculation of the sap flow. Temperature differences were measured every 10 s and recorded every minute by a UNILOG data logger (EMS, Brno, Czech Republic).

Infrared Imaging. The infrared camera (model 600 IR Imaging Radiometer from Inframetrics, 1990) with temperature resolution of 0.1 °C, spectral band-pass 8–12 μm , and detector HgCdTe at 77 °C was cooled by liquid nitrogen. The camera was mounted on a tripod and focused on the smoothed xylem surface to take heat field images (Figure 1, lower panel). No filters were used, but a silicon zoom lens was applied. The temperature scale was about 4 °C within the range 15–22 °C. Several hundreds of IR images were taken periodically. The actual terms of recording were selected in correspondence with the continuous record of the sap flow.

General Considerations. According to physical technical reasoning, evaporation E per unit time and area should be equal to the product of the water potential gradient ($\Delta\Psi = d\Psi/dx$) (or humidity gradient) of the phases concerned with a proportionality constant, the evaporation number s (with the units $\text{kg}/(\text{m}^2\text{h})$)

$$E = s \frac{d\Psi}{dx} = s \text{ grad } \Psi \quad (1)$$

In the physiological literature, the evaporation is identified with the volume flux density of water (J_v), and the evaporation number s with the water conductivity coefficient (L).³ If this is the case, how can then the part of the crown of a tree that is exposed to sunshine evaporate or transpire up to 10 times as much as the shaded part of the same tree?¹⁶ As continuous recordings demonstrate, only modest temperature differences and variations in water vapor pressure deficit are noticed when sunshine and shadows are alternating. Why do some trees (e.g., Norway Spruce) show high transpiration rates at only 8 °C when ordinary open water only modestly evaporates? Why does less than 5–8% of water turnover occur between sunset and sunrise despite sometimes still reasonably high ambient night temperatures?¹⁷

Why is then direct sunshine so favorable for evaporation and water transport? There may be a very efficient coupling mechanism between incident solar energy converted into heat and tensile water evaporation from leaves. Technically, heat transfer Q per unit area and time is related to the temperature gradient dT/dx and the heat transfer number λ ($\text{kcal}/(\text{m}^2 \text{ } ^\circ\text{C})$) via (c_p is the specific heat of humid air, c a proportionality constant)

$$Q = cc_p E = \lambda \frac{dT}{dx} = \lambda \text{ grad } T \quad (2)$$

If evaporation and heat transfer are efficiently coupled so that essentially all heat is dissipated through evaporation, which has apparently been approached by evolution for illuminated leaves, then $s = \lambda/c_p$ (which implies that $\text{grad } T = c \text{ grad } \Psi$) and

$$E = \frac{Q}{\text{grad } T} \frac{\text{grad } \Psi}{cc_p} = \frac{Q}{cc_p} \frac{d\Psi}{dT} \quad (3)$$

This relation first explains why at lower ambient humidity (higher $\text{grad } \Psi$) less light (solar heat Q) is required by trees to reach maximum transpiration.¹⁷ It also suggests that a high rate of evaporation would require a high gradient of the water potential with respect to temperature. But to understand why considerable variations in transpiration are found in trees with comparable air temperature, humidity, wind velocity, and abundant soil water, eq 3 must be more complicated and inherently highly nonlinear. More specific, $d\Psi/dT$ in eq 3 should be a nonlinear function. This function may depend on the concentration of hydrogen bonds activated during transition to the tensile state of water.

Theoretical Evidence for Nonlinearity. This conclusion may help us to describe the research problem. It is well-known that new phenomena may occur far from equilibrium due to self-organization. An example is the Benard instability.¹⁸ When a layer of viscous liquid is heated on a plate so that an increasing temperature gradient develops across this layer, heat transfer first increases proportional to the temperature difference (as predicted by eq 2 on the basis of a constant heat transfer number λ). A further increase in the temperature difference leads however to a drastic change. Regular convection cells start developing in the liquid, and the transfer rate for heat Q drastically increases. The heat transfer coefficient λ thus changes to $\lambda = \lambda(Q)$, and eq 2 becomes nonlinear. Something similar may happen with the evaporation of water from leaves (eq 2) so that $\lambda = Q/\Delta T_d$, with ΔT_d = temperature distance across d , or other quantities become nonlinear: $\lambda = \lambda(Q)$, $\Delta\Psi = \Delta\Psi(Q)$, $c_p = c_p(Q)$. A much more efficient coupling of solar heat to evaporation of water under tensile strength in plant water conduits may thus become possible. Since the available heat Q is determined by the incident solar radiation what could, for example, happen is that the distance d across which the temperature gradient is effectively applied would narrow down to provide a more efficient heat transfer in combination with a minimized heat capacity. This could occur via some self-organization process of the tensile strength water–plant cell environment within the parenchyma of leaves.

It is known that water enters the foliage through vessels from where it spreads over cell walls and across cells of the mesophyll. It has a very high surface area (about 10–20 times the leaf surface) made up of a dense network of cellulose fibers separated by 7–10 μm thin capillaries. As long as water creates a film over this structure, there is no sap flow movement in the vessels below. Energy of evaporation is not efficiently transduced into hydromechanical energy of tensile strength water. But as soon as this water evaporates so that the water level drops into the capillaries or into the pores of membranes, the sap starts to move, and solar energy is converted into mechanical energy. Evaporation of water via solar energy (Q) may thus become very efficiently nonlinearly coupled to a thin capillary tensile water film or tensile water in the pores of cell membranes. In a simplified picture, the effective thickness (d) of the layer, across which the temperature gradient ΔT_d is provided for heat transfer, may decrease in dependence on the solar energy supply

$$\Delta T_d \rightarrow \Delta T_d(Q) \quad (4)$$

Alternatively, the evaporation number $s = \lambda/c_p$ may increase. This would make evaporation as expressed by eq 3 nonlinear so that the energy throughput may increase like in the Benard phenomenon when convection cells begin to self-organize.

If one intends to show that water evaporation from trees is indeed a nonlinear phenomenon, then one has to concentrate

on intermolecular interactions between water molecules and of water molecules with water conduit—parenchyma interfaces. It was mentioned that already “normal” water is known to contain a significant proportion of water molecules held mostly together by hydrogen bonds. In water, hydrogen is covalently attached to oxygen within one water molecule (about 492 kJ mol⁻¹) but is subject to an additional attraction (about 23.3 kJ mol⁻¹) to the oxygen atom of a neighboring water molecule. This so-called hydrogen bond interaction, which is approximately 90% electrostatic and 10% covalent, exceeds by almost 10-fold the energy involved in thermal fluctuations, but bonds are only short-lived and involved in steadily changing “flickering cluster” interactions. Hydrogen bond dynamics in hydrogen-bonded water networks include cooperative and anticooperative phenomena. By increasing its electron density in its “lone pair” region, a hydrogen-bond-donating molecule increases its acceptance for further hydrogen bond contributions. The opposite is true for hydrogen bond accepting water molecules. Physical chemical parameter changes and additions of ionic and molecular species may drastically influence hydrogen bond dynamics and energetics. When the water structure expands in supercooled water or in ice to a more open structure, more hydrogen bonds are activated, and the hydrogen bonds in (hexagonal) ice are stronger by 3 kJ mol⁻¹ compared to water.

For a comprehension of the dynamics and energetics of tensile water, we need theoretical approaches that consider intermolecular bonding including its nonlinearity and cooperativity. An interesting phenomenological approach to the problem, even though it is traditionally not used in water transport physiology, is the well-known classical van der Waals (VdW) equation. It is the simplest (empirical) equation that considers the role of intermolecular forces in the physical chemistry of water. It has also shown to be practically useful. For our effort, we will stick to the simplest equations possible, which still express the required properties, in our case the nonlinearity of intermolecular bonding in dependence of intermolecular distance. The VdW equation fulfills this condition. It has already been proposed to be a key factor for understanding tensile water strength and tensile water dynamics in relation to forest decline due to pollution.¹⁹ But disturbed tensile water dynamics in trees has not yet been considered seriously as a source of forest decline, probably because of a lack of understanding of tensile water properties. The VdW equation has the following structure (p = pressure, V = volume, R = gas constant, n = number of moles involved, T = temperature)

$$(p + p')(V - b) = nRT \quad (5)$$

with $p' = a/V^2$ for phase transitions of water and real gases. It considers the chemical interaction between molecules by adding a pressure term p' to the pressure variable. This term considers the cohesion pressure, which depends on the tensile state, and the volume V that the water molecules occupy. It also considers, through b , that molecules also occupy a certain volume (covolume) by themselves. A pressure–volume presentation for the behavior of real water molecules according to the VdW equation is shown in Figure 2. It actually shows that water expanding toward the vapor phase can develop tensile strength. A deep minimum of negative pressure is visible before the state of water approaches the gas phase at ambient pressure and large molar volumes V . The VdW equation is, of course, a simplified approach aimed at considering intermolecular bonding between water molecules. Any theory on tensile water dynamics has to consider intermolecular bonding. In reversible thermodynamics, negative pressures are simply considered to be nonphysical; the

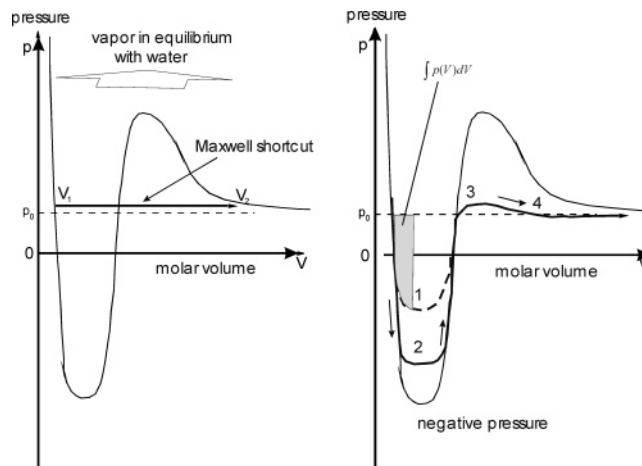


Figure 2. Pressure–volume diagrams showing the characteristic performance of real water/gas phases as described by the empirical van der Waals equation. The left panel shows the pathway at ambient pressure p_0 , along which ordinary (nontensile) water is expected to evaporate. The right panel shows the paths (1 and 2) along which tensile strength water is building up a “negative” pressure, before it is converted into tensile, adsorbed water at ambient pressure for evaporation (paths 3 and 4)

van der Waals equation is only used to indicate possible metastable states such as those of overheated liquids or oversaturated vapor. Usually, evaporation of ordinary water is expected to follow a shortcut along the environmental pressure line (Figure 2a) to satisfy the Maxwell criterion of equal areas below and above the horizontal shortcut. Textbooks typically only regard such a pathway as realistic, since the Maxwell criterion essentially claims that entropy can be considered as a quantity of state, which is a fundamental assumption of reversible thermodynamics. It is assumed that the entropy of the water/vapor system can be defined irrespective of its history during a thermodynamic process. Under tensile strength conditions, water is however more ordered and should have less entropy than ordinary water. The entropy of water should therefore depend on whether tensile strength could build up or not. Tensile strength must therefore be considered.

Provided that tensile strength can build up, the van der Waals equation readily explains and describes this property of water; when molecules are pulled apart, a pressure below ambient pressure p_0 is reached (curve section 1 in Figure 2b). This pressure can further decrease to reach pronounced negative values (curve section 2 of Figure 2, right panel). Computer simulations show that when the value for b in the VdW equation is maintained (as determined at the critical pressure) but the cohesion parameter a (atm L² mol⁻²) is changed from 3 to 3.5 and 4, the pressure minimum p_{\min} can be varied from -0.3 to -18 and -38 MPa. When the expansion is sufficiently large, the negative pressure is not any more sustained (curve section 3) and approaches the vapor phase at ambient pressure. It will depend on external conditions, such as the energy input or the environment’s ability to sustain negative pressures, whether a (1) shallow or a (2) deeper tensile strength curve is followed.

It is immediately evident that water following a negative pressure (or tensile strength path) towards the vapor phase and thus toward a more negative water potential is able to perform work. It is equivalent to the area, which the negative pressure curve is including below the ambient pressure line p_0 . The molecular interaction term p' in the van der Waals eq 5, when applied to tensile water in tree water conduits, will of course also include the interaction of water with the surface of the xylem capillaries, so that a somewhat extended van der Waals

equation will have to be applied. The quantity p' will have to be replaced by a more elaborate quantity p'' , which will also depend on the height of the sap column in the tree. It is not the aim and not necessary for this contribution to provide a detailed formula for it.

Before further discussing the VdW equation, let us indicate that it can be written in the form

$$V^3 - V^2\left(b + \frac{nRT}{p}\right) + \frac{a}{p}V - \frac{ab}{p} = 0 \quad (6)$$

Since the water/vapor volume nRT/p that is of interest to us is always significantly larger than the minimum covolume b of water, eq 6 can slightly be simplified to

$$V^3 - V^2 \frac{nRT}{p} + \frac{a}{p}V - \frac{ab}{p} = 0 \quad (7)$$

This eq 7, as a thermodynamic relation, appears to tell us under what conditions water, via the tensile water state, will convert into vapor, but it does not tell us anything about the mechanism involved and the rate of the reaction. For this, we need a kinetic mechanism, which is compatible with eq 7, that respects the thermodynamic constraints.

Kinetic Relation for Tensile Water Behavior. Let us assume that water molecules can get involved in different degrees and types of intermolecular bonding. Depending on their statistical interaction with surrounding molecules, transient clusters and networks of specifically interacting water molecules will form. It is, for example, known that intracellular water close to any membrane or organelle is organized differently from bulk water. If mechanically pulled or if molecules are extracted due to evaporative processes, then the water structure will change and become asymmetric with increasing hydrogen and van der Waals bonding distances in the direction of the pulling force. Water molecules subject to such conditions will be called tensile water molecules. Nontensile water will contain a negligible amount of tensile water molecules; tensile water will contain a variable concentration up to a maximal concentration of tensile water molecules.

What would an interrelation between ordinary water molecules (here we call them A), tensile water molecules (here we call them V' , because the molar volume V of water will increase with an increasing concentration of water molecules involved in tensile interactions ($V' \approx V$)), and water vapor (here called B) look like? Again, we will try to derive an equation that is as simple as possible. What kind of kinetic equation do we expect? Since at least two tensile molecules have to interact from opposite sides with a nontensile molecule to transform it into a tensile, stretched one, a third-order equation appears to be the simplest approach. It may be described as follows.

The global reaction for tensile water buildup and evaporation in trees may be written as



Figure 3 shows our proposal for the involvement of tensile state water (named V' for reasons which will become clear later, because two equations will be compared) in this process. It is supposed that clusters or aggregates of water under tensile state with activated intermolecular hydrogen bonding will form or dissolve. Since tensile water is associated with a decreased or even negative pressure, ordinary water molecules will be attracted. The overall energy for this process will of course be supplied by solar evaporation, which is evaporating water

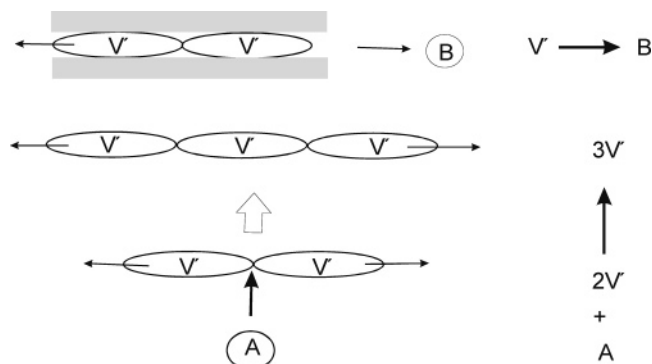
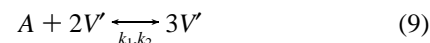


Figure 3. Reaction scheme showing the assumed interaction kinetics between ordinary water molecule (A , shown as a sphere) and water molecules exposed to tensile strength (V' , shown as stretched ellipses). A is attracted due to the lower, "tensile" pressure and stretched by two tensile water molecules V to become a tensile molecule itself. Figure 3 (top) visualizes the evaporation step of tensile water molecules to water vapor molecules (B).

molecules while placing others under tensile conditions. When they are engaged in tensile interactions, two tensile molecules ($2V'$) may pull an ordinary water molecule A in to yield an additional third tensile molecule ($3V'$). In molecular terms describing the hydrogen bond dynamics, such a mechanism may indicate that two molecules engaged in hydrogen-bond-mediated tensile bonding may involve a third, ordinary water molecule in activated hydrogen bonding. In this reaction step, a molecular feedback is described that actually is evident in the hydrogen bond dynamics: A molecule that has induced a hydrogen bond with another water molecule to include it in tensile interaction encourages additional hydrogen bond interaction. That is, it may include an additional water molecule into the tensile structure. A reverse reaction would mean that a tensile water molecule would escape the tensile water structure to become a regular water molecule A



Another way of escape for tensile water would be the evaporation process, which proceeds in the leaves, where tensile water molecules (V') are reaching the gas interface. Here, a direct transition into the gaseous state (B) can be expected (compare Figure 3). Such a reaction step from tensile water to evaporated water will be necessary to sustain the expected energy conversion process



The rate equation for V , the tensile water, from eqs 9 and 9a, then reads

$$\frac{dV'}{dt} = -k_2 V'^3 + k_1 A V'^2 - k_3 V' + k_4 B \quad (10)$$

and the rate for the evaporation of tensile water (when the reverse condensation is neglected) is consequently

$$\frac{dB}{dt} = k_3 V' \quad (11)$$

We will now first investigate whether this kinetics makes sense and whether it is really related to the thermodynamic VdW eq 7. It has to be shown that both equations express the same system and that the kinetic behavior is in line with what we know about the thermodynamics of water. We have, before all,

to test whether the molar volume behavior of tensile water is consistent with expectations from the VdW eq 7, which considers intermolecular forces, as they behave during the transition from ordinary water to tensile water and water vapor. For this purpose, we will examine the steady-state situation for rate eq 10 setting $dV/dt = 0$. It is determined by the equation

$$V'^3 - V'^2 \frac{k_1 A}{k_2} + \frac{k_3}{k_2} V' - \frac{k_4 B}{k_2} = 0 \quad (12)$$

Now it becomes clear why we named tensile water molecules V' . The more water molecules involved in the tensile state, the more volume they occupy and consequently the larger the molar volume V of water: $V' \approx V$. The concentration of tensile molecules is proportional to the molar volume of water. Steady-state kinetic eq 12 should therefore be directly comparable and equivalent with the van der Waals eq 7. In fact, comparison with the VdW eq 7 shows that it is identical when the thermodynamic VdW factors nRT/p , a/p , and ab/p are identified with the kinetic factors $k_1 A/k_2$, k_3/k_2 , and $k_4 B/k_2$ of eq 12

$$\frac{nRT}{p} = A \frac{k_1}{k_2} \quad (13a)$$

$$\frac{a}{p} = \frac{k_3}{k_2} \quad (13b)$$

$$\frac{ab}{p} = B \frac{k_4}{k_2} \quad (13c)$$

This identity may still be coincidental and arbitrary since eq 7 is a thermodynamic relation, and eq 12 a kinetic one. Since the concentration of tensile molecules V' could be related to the molar volume V (for this reason the concentration of tensile molecules was named V'), it has therefore to be shown that the kinetic parameters on the right side of eqs 13a–c have a thermodynamic meaning, like the parameters on the left side. It is seen from eqs 13a–c that the parameters on the right, which means the coefficients from the kinetic eq 12, involve concentrations (A and B) and ratios of reaction constants, which can be expressed as ratios of concentrations. We are dealing with equilibrium constants K_{eq} , which are independent of activation energies and related, as well-known, to the free energy of the reaction involved: $\Delta G^\circ = -RT \ln K_{eq}$. It is thus demonstrated that eq 12 has a thermodynamic meaning, and since a third-order equation explaining the variation of the molar volume $V' \approx V$ is given, the same phenomenon should be described as with the empirical VdW eq 7.

From this, by comparison of eqs 7 and 12 it follows that formally the thermodynamic quantities p , a , and b can be related to the following kinetic parameters $p = k_2$, $a = k_3$, and $b = k_4 B/k_3$.

Interestingly, the thermodynamic (or tensile) pressure p of the VdW equation is related to the rate constant of the autocatalytic reverse reaction step (eq 9), which indeed involves intermolecular interaction (Figure 3a). The cohesion pressure factor a is related to the (solar) evaporation rate constant k_3 , which energetically leads to the buildup of the tensile state. The smallest covolume b is correlated with kinetic factors containing the evaporation equilibrium constant and the water vapor concentration B .

Equations 9 and 9a, which have led to steady-state eq 12, are formally equivalent with the so-called Brusselator reaction. Nicolis and Prigogine have pointed out²⁰ that this reaction

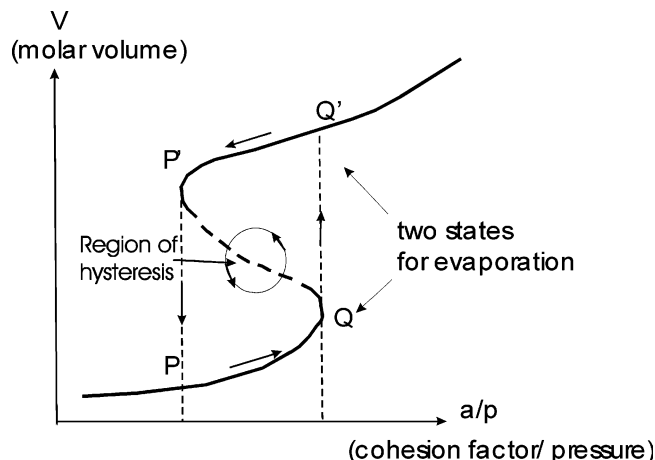


Figure 4. S-shaped curve of V (concentration of tensile water molecules or molar volume) versus a/p (cohesion pressure factor divided by pressure) explaining stable (PQ and $P'Q'$) branches and the unstable, dotted (QP') branch as well as the region between a_1/p and a_2/p where hysteresis will occur.

shows a surprising analogy to the empirical van der Waals equation for phase transitions, if the variable V engaged in autocatalysis is identified with the molar volume of water and another variable parameter, $k_4 B/k_2$, the last term in eq 12, with the pressure p . However, a comparison with eq 7 shows that this is not entirely correct. This term is not a thermodynamic pressure but the quantity ab/p . Considering that b , the covolume parameter, is a constant, then this variable is proportional to the ratio between the cohesion pressure constant a and the measured pressure p . When a , the cohesion pressure constant, is zero, we are dealing with an ideal gas. When it is a large, we are dealing with a highly cohesive molecular system, which can be stretched. The ratio a/p must consequently be of special interest for the buildup and description of tensile water. It apparently describes the buildup of tensile strength, in terms of mobilizing intermolecular bonding via the cohesion pressure constant a , with increasing distance from equilibrium, when the VdW curve first leads to negative pressure, and then, at high molar volume, again approaches ambient pressure (Figure 2). It is interesting to note that according to eq 13b a/p is equivalent to the ratio k_3/k_2 . This is the ratio of the rate constant for evaporative extraction of water (k_3) to the rate of the autocatalytic reverse reaction (k_2), during which tensile molecules are again escaping from the structure of tensile water. This makes sense; the larger k_3 and the smaller k_2 , the larger the buildup of the tensile state of water, pushing the system away from equilibrium. This confirms the conclusion that thermodynamic eq 7 and kinetic eq 12 are equivalent and related.

When eq 12 is investigated and V' , which is proportional to V , is plotted versus $k_4 B/k_2$, which is proportional to the ratio a/p , a region of S-shape is observed as shown in Figure 4 (and discussed for the Brusselator equation in ref 20 with $k_4 B/k_2$ being interpreted as pressure p). It allows a “multiple state” situation between a_1/p and a_2/p with the stable branches PQ and $P'Q'$ and an unstable branch QP' between (compare to ref 20). Because of eq 11, which relates the evaporation of tensile water to V' , the concentration of tensile water molecules, this means that the rate of evaporation increases in a nonlinear way along the S-shaped curve. This is a similar situation, as initially explained for the hydromechanical Benard system, when the heat flow starts increasing through self-organizing convection cells. Here, evaporation is controlled and enhanced through self-organization of tensile water. We are dealing here with a solar-powered irreversible thermodynamic mechanism.

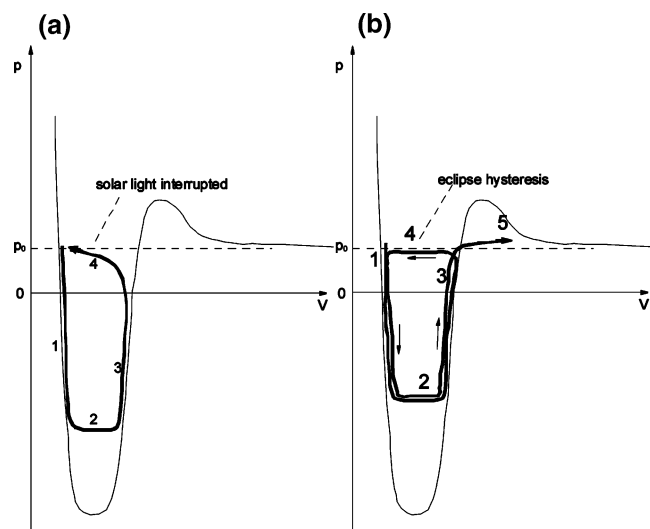


Figure 5. Pressure–volume diagrams showing the characteristic performance of real water/gas phases as described by the empirical van der Waals equation. (a) The buildup of tensile strength (paths 1, 2, and 3) during solar evaporation and its breakdown (path 4) during interruption of solar irradiation is explained. (b) The whole hysteresis cycle expected during interruption of solar radiation is depicted, leading to a breakdown of tensile strength (paths 1, 2, 3, and 4) and its recovery along paths 1, 2, 3, and 5.

It is clear from the mathematical situation shown in Figure 4 that states from branch PQ may jump to states on branch $P'Q'$, provided that they receive a sufficient perturbation. The system is thus intrinsically excitable, when the system is pushed so far from equilibrium that this multi-steady-state region is reached. In addition, it is of course also subject to a hysteresis, when a/p varies in the region of multiple states. When the energy input is increased, the system is first pushed along PQ , then near Q will make a transition near Q' before continuing along this branch. When the energy input is decreased, the system will move back along the $Q'P'$ branch before making a transition to P near P' . When energy input is further decreased, evaporation will further decrease following the lower branch. All together this means that a hysteresis of a specific volume of water V may arise in a certain region as the cohesion/pressure ratio varies between a_1/p and a_2/p .

Since the evaporation rate dB/dt described by eq 11 depends on the concentration of tensile water molecules V' and thus on the molar volume of water V , as described by the S-shaped curve in Figure 4, a hysteresis of evaporation and two different rates of evaporation of water from leaves under identical solar energetic conditions is therefore indeed to be expected. When solar light intensity, which is ultimately responsible for water transpiration and the buildup of tensile strength water in trees, is increasing or decreasing, reflecting increasing or decreasing a/p ratios, different evaporation pathways PQ and $Q'P'$ may therefore be followed.

Let us examine this situation closer in the pV diagram, in which the van der Waals equation is typically presented (Figure 5). In the left panel, it is shown how ordinary water may be transformed into tensile strength water in a tree, which develops along pathways 1, 2, and 3. Let us now assume that solar light and thus the driving force for tensile strength conditions is again decreasing. In this case, the water will again approach its ordinary state. It will thus return into the ordinary state along pathway 4. Water would have behaved like a rubber tape, which is again relaxed. Work would have been temporarily performed and energy stored to be subsequently released as heat. Water molecules engaged in such a loop will not contribute to a

conversion of solar energy into work. When solar light returns again, tensile strength may be again built up along paths 1, 2, and 3, but the condition of water may then continue to change along path 5 towards evaporation at ambient pressure (Figure 5, right panel). Such a process would correspond to a rubber tape, which is continuously pulled to perform work. If, during this tensile water evaporation, as shown in Figure 4, the ratio of cohesion parameter to pressure (a/p or k_3/k_2) is increased to reach the triple state region (intermediate state unstable), a high rate of evaporation corresponding to the branch $P'Q'$ and eq 11 may be reached. This is the supposed dynamic operation mode of the solar-energy-powered vapor machine of trees. But depending on whether the driving force (solar intensity) is decreasing or increasing, the evaporative system is thus also forced into an opposite hysteresis loop. Within this loop, entropic energy (heat) is being produced without effective work. The area enclosed by loop $PQQ'P'$ is a measure for it.

Sap Transport Studies in Trees during an Eclipse. There is presently no artificial system that can sustain the tensile state of water for a sufficiently long time to perform an experiment on tensile water evaporation. Our interest was therefore to test this straightforward model on nonlinear solar-energy-mediated sap evaporation from trees, taking advantage of the solar eclipse of August 11, 1999. Since the eclipse in central Europe occurred at noon time, the solar evaporative process in trees was expected to be in a dynamic steady state where the buffer capacity for water storage is not dominating the response to changes in solar radiation. It is known that a willow tree may use approximately 1% of its trunk volume temporarily as a water reserve, an amount equaling 3% of daily water loss.¹⁶ For this reason, sap flow measurements were planned for different trunk elevations. The eclipse provided quite favorable preconditions for the experiment; during a solar eclipse, the spectral and spatial distribution of solar radiation as well as air flow and humidity are expected to remain the same in contrast to shadowing of trees by clouds or operating mirrors, meshes, or filters in the immediate surrounding. Of course, one could also think of performing such experiments with artificial shading of a tree, for example, using a fine mesh handled from a crane or another mechanical structure exceeding the size of a tree. In this case, special care would have to be taken not to change significantly ventilation, humidity, and air flow around the tree because this could drastically affect water evaporation from trees, which is monitored. Since, in the regions of experimentation, Berlin and Sobesice near Brno, the eclipse was only 90%, there was enough light to keep the leaf stomata open, which are known for their high light sensitivity. A photon flux density of only approximately $1 \mu\text{mol m}^{-2} \text{s}^{-1}$ is needed to keep the stomata open, compared with a much higher flux of visible solar light photons of around $2000 \mu\text{mol m}^{-2} \text{s}^{-1}$ (420 W m^{-2}) and $150 \mu\text{mol m}^{-2} \text{s}^{-1}$ (420 W m^{-2}) in the ultraviolet region available on the earth's surface.²¹ Even in the region of total eclipse around Munich, Germany, during the same event, a distinct stomata closure was not observed due to the relatively short duration of this astronomical phenomenon.²² The absence of stomata closure in our experiments is also supported by the observation of the sap flow hysteresis in different tree species.

If, during increasing and decreasing eclipse, evaporation (sap transport) in trees would follow a linear dependence reflecting a constant evaporation number of $s = Q/(dT/dx)cc_p$, proportional to the molar volume of water, resulting in a sap flow strictly proportional to the solar energy input, then we would deal with a conventional evaporation mechanism, and no hysteresis would be observed. Such a mechanism is assumed in textbook

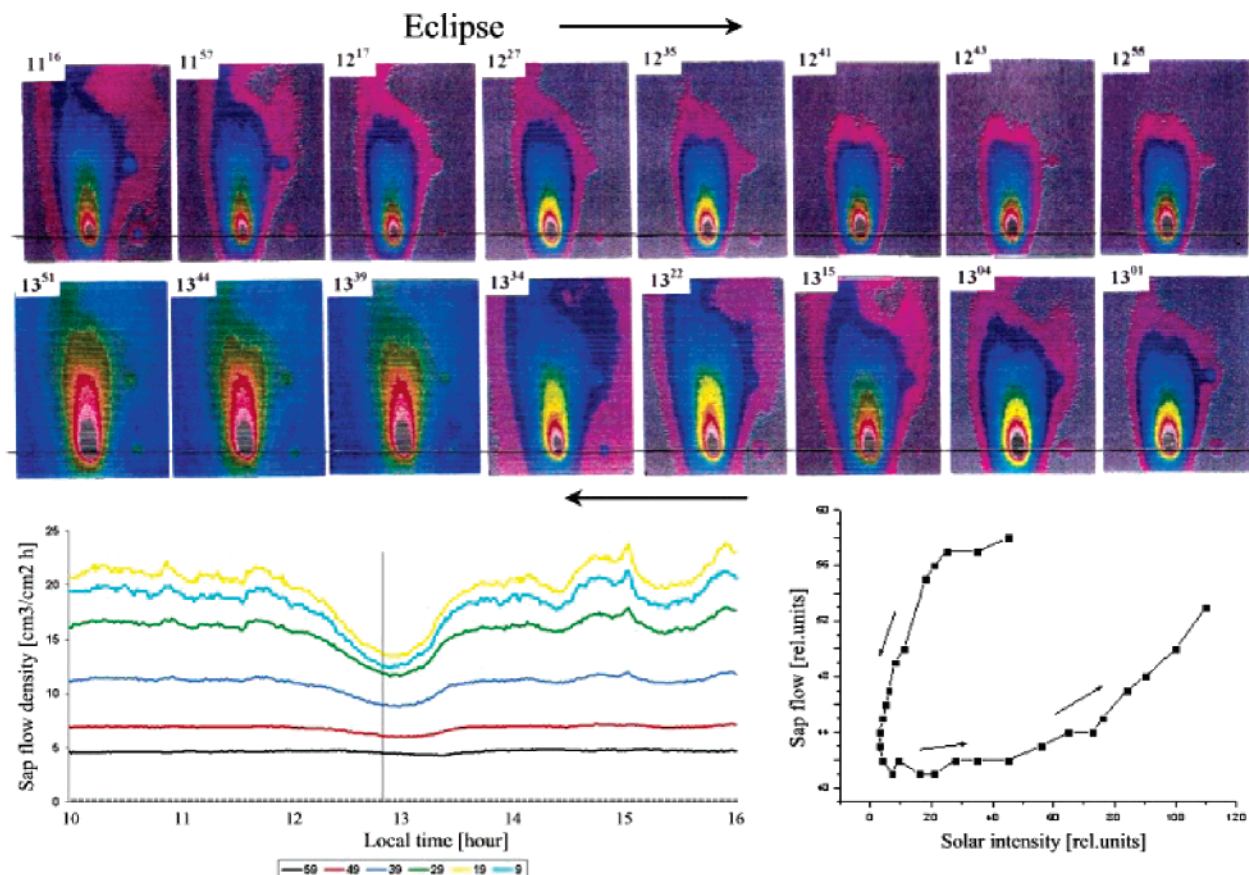


Figure 6. IR sap flow images (top panel) and sap flow rates (lower-left panel) for a lime tree during the solar eclipse at Berlin. The ambient and tree trunk temperature increased by approximately 1.5 °C between 11.21 a.m. and 2:02 p.m., corresponding to a shift from red to green or black (trunk) to blue. The sap flow dynamics, recorded by a radial sensor, are shown for different xylem depths below the cambium (marked in legend by numbers in millimeters). Sap flow in dependence of solar energy input during the solar eclipse showing clear hysteresis (lower right panel).

experiments when the van der Waals curve is horizontally short cut at ambient pressure to allow a coexistence of water and vapor proportional to the magnitude of the specific molar volume. If, in contrast, one finds a clear hysteresis for decreasing and increasing solar intensity values, then one is dealing with an S-shaped nonlinearity as to be expected from a self-organization process as explained above (Figure 4) and expected as a straightforward consequence from the kinetic version (eqs 9 and 9a) of the van der Waals equation. As long as, with decreasing Q and a decreasing temperature gradient dT/dx in the evaporating parenchyma tissues, the heat-transmitting, self-organized layer is maintained, the evaporation process will follow a more efficient kinetic mechanism, as explained by eq 11 with the upper branch of the S-shaped curve along Q' , P' , and P of Figure 4. However, if the layer is finally deactivated, then the evaporation process toward tensile strength conditions will only gradually improve again with increasing solar light intensity along P , Q , and Q' , as explained in Figure 4.

Figure 6 shows how sap flow and infrared images changed during the eclipse at Berlin. The iso-temperature profiles around the heated needle describe ellipses, with the heat source in the focus and with the eccentricity determined by the sap flow, which transports the heat. How these infrared images of heat fields can be obtained and can be used to deduce new information about sap flow has been explained in publications.^{23,24} The eclipse started at 11:21 a.m., its maximum was at 12:42 p.m. (vertical line in Figure 6, lower-left panel), and its end was at 2:02 p.m. It can be seen how, during the eclipse, the heat field around the linear heater was changing, simultaneously with a shift in the ambient temperature of the tree trunk.

The sap flow in the tree clearly drops during the eclipse; however the response is asymmetric. A plot of the solar energy input versus the measured sap flow rate in the lime tree (Figure 5, lower-right panel) shows that the recovery of sap flow is clearly delayed behind the recovery of solar radiation.

Figures 7 and 8 compare the solar energy input and the corresponding sap flow rate in maple and lime trees measured during the same eclipse in Sobesice at the base of the tree and at 11 m (maple) and 12.6 m (lime) height under the crown. The impact of the eclipse is again clearly seen. But while the solar radiation decrease coincides with the decrease in sap flow rate, it again clearly lags behind the renewed increase in solar intensity. Remarkably, the measured sap flow rate decreased by a factor of 2–3. A similar striking decrease by a factor of 2–3 of the transpiration rate of trees on light intensity was, by the way, also observed in Denmark during the nearly total eclipse of June 30, 1954, with negligible humidity change and a temperature decrease not larger than 2 °C.¹⁷ This emphasizes the optimized utilization of absorbed solar heat Q for evaporation as indicated by eq 3. Plots of the sap flow versus solar energy input during the eclipse for both “under crown” and “base” sap flow measurements at Sobesice (Figures 7 and 8, right panels) show a clear hysteresis for both cases (similar to that observed with the lime tree in Berlin, Figure 6). So, a hypothetical stored water volume in the trunk itself cannot be responsible for it.

The visualization of the heat field as an IR image allowed us to perform an experimental test, which is very instructive for the understanding of the correlation of solar evaporation with sap transport in the tree trunk. If the sap is “pulled” by evaporation, as the cohesion–tension explains, then cutting

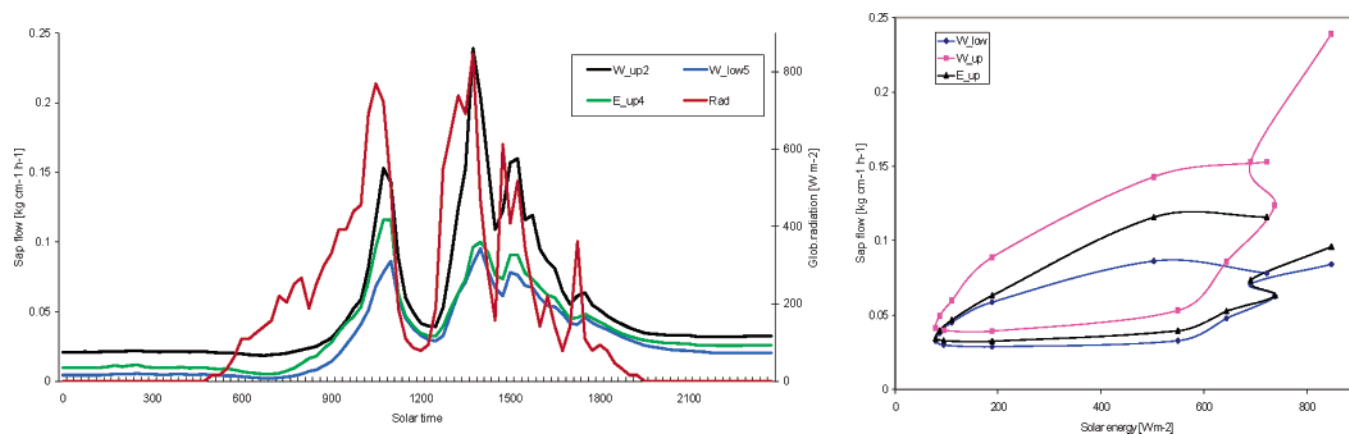


Figure 7. Comparison of solar energy input during the day of the eclipse and the impact on sap flow in a maple tree measured in Sobesice at breast height from the western side of the stem and at a height of 10 m (marked “up”) from the western and eastern sides of the big branch.

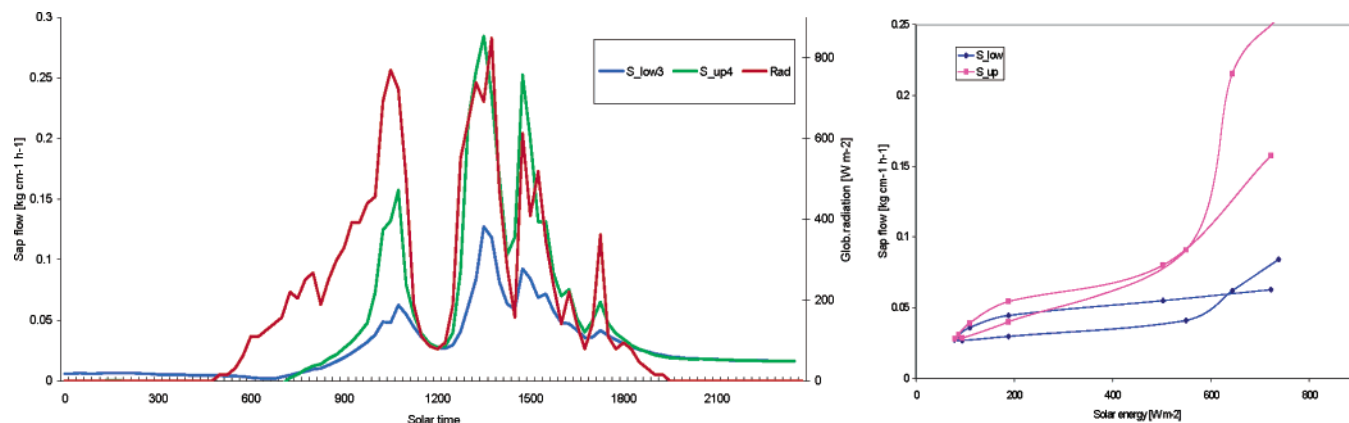


Figure 8. Comparison of solar energy input during the day of the eclipse and the impact on sap flow in a lime tree measured in Sobesice at breast height from the western side of the stem and at height of 10 m (marked “up”) from the western and eastern sides of the big branch.

xylem pathways above should stop sap flow. Experiments were performed where infrared images were taken parallel to a heated needle in the tree trunk (picture on the right in Figure 9), so that the effect of heating of sap water could be observed across the tree cross section. They allowed us to clearly recognize two areas within the tree profile where high sap flow rates were observed (Figure 9). They correspond to the xylem regions below the bark, where sap flow occurs. When the lime tree trunk was cut above the sensor area down to the pith, the corresponding temperature peak reflecting xylem sap flow began to decrease within seconds, so that an asymmetrical temperature pattern is formed (lower IR profile). Flow in the other not damaged half of the stem continued in the meantime without changing. The same fast reaction on severing one-half of the stem was recorded also by sap flow sensors (Figure 9, top panel, actual time in hour and minutes). This experiment confirms in a convincing way that sap water is actually pulled as tensile water up the tree by evaporation in the leaves. It also shows that the time response for stopping sap flow in the tree trunk is quite fast. This is to be expected when the sap is pulled. This experiment shows that for the sap flow experiment, performed at noon, a reasonably fast response (faster than 1 min) can be expected for a change of evaporative water loss in the crown.

The fast-responding tensile state of water in trees can also be shown by additional experiments. We studied the reaction of sap flow on loading tree roots by heavy machinery in the forest or cutting roots (Figure 10). Two types of reaction are demonstrated here:

(1) A sharp increase of flow is observed on cutting the roots due to an abrupt release of root–soil resistance below the cut

end. Water can now move reasonably freely controlled by the hydrodynamic resistance in the remaining part of the water-conducting elements.^{15b–c,25} This type of reaction also confirms the pulling effect of evaporation and the tension in the water columns.

(2) Repeated mechanical loading of the soil surface during tractor moving caused the increase in flow in roots and stems in all xylem layers.²⁵ Water is probably forced to move from the affected point in direction of the sprouts but to some extent also in the direction of the roots, when roots are compressed somewhere along their length. It behaves like an elastic medium. The mechanical forces, holding back tensile strength water columns, are thus suddenly partially compensated, allowing tensile water to be faster pulled by evaporation. This is seen in the temporary increase in sap flow during mechanical loading of roots (Figure 10). Also this response testifies for a rapid communication of forces along tensile strength water pathways.

Sap flow rates in the stem of the treated spruce tree and in one coarse root, which were mostly connected to treated roots, were determined. Vertical lines indicate periods of tractor moving (during loading experiments) and root severing.

Discussion

A kinetic model was developed to describe the tensile behavior of water. It was shown to be mathematically in agreement and related with the Van der Waals equation in terms of the pressure-dependent molar volume behavior of water and to involve autocatalysis, as expressed in the kinetic Brusselator-type reaction. Solar-energy-mediated interaction between tensile

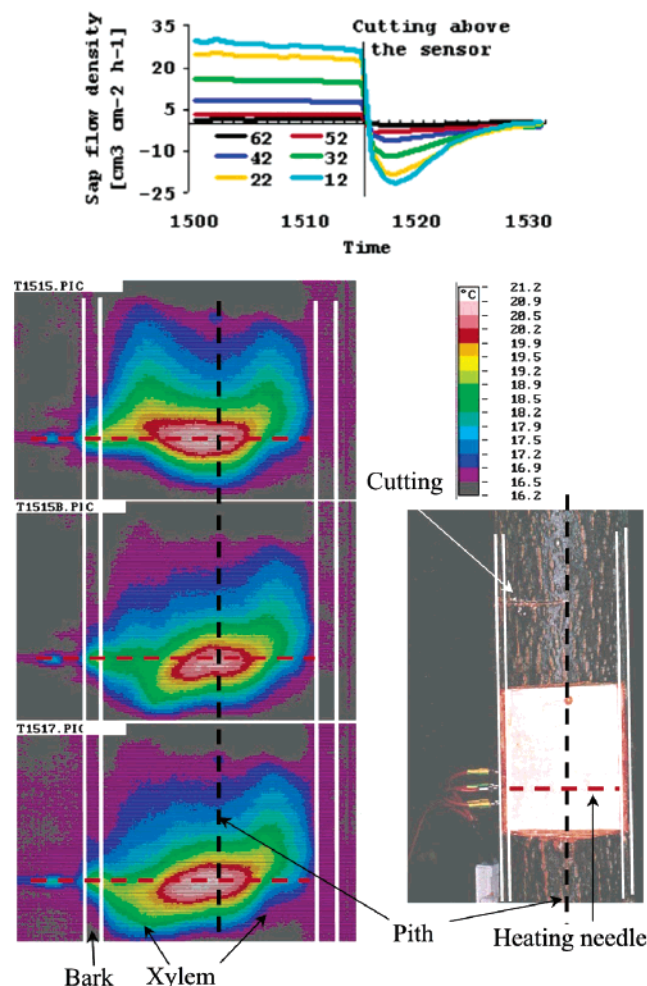


Figure 9. Sap flow measured by the HFD sensor in different xylem depths (top panel, numbers correspond to the xylem depth below the cambium in millimeters) and infrared images visualizing the sap flow in a tree trunk heated by a horizontally introduced heating needle (middle panel). The fast sap flow in the xylem regions is clearly seen (top image). When the tree trunk was cut 20 cm above the heating needle down to the pith (right panel), the sap flow in the affected xylem structure reacts within seconds (sap flow data and middle and lower images). This proves that the sap is pulled and sap flow reacts fast to changes in evaporation. Both the sap flow and the IR images demonstrate that the highest reaction was observed in xylem depth where the sap was pulled with a higher force.

molecules (water involved in tensile hydrogen bonding) activates more tensile interaction (activation of additional water molecules involved in tensile interaction). Displacement of the molecular system from equilibrium and access to nonlinear phenomena are therefore to be expected. The performed experiments demonstrate a pronounced hysteresis in tensile water evaporation. It is in agreement with the derived kinetics (eqs 11 and 10) and the bistable state reached for the molar water volume far from equilibrium (Figure 4).

The area included by the eclipse-induced sap flow hysteresis loops shown in Figures 7 and 8 (sap flow per area times energy per area) has the dimension of flux (J) times force (F) per volume. It consequently expresses a change in entropy production σ between the decreasing and increasing eclipse phase or the change between two different states of entropy production σ per volume, which in general form can be described as²⁰

$$\sigma = \sum_k J_k F_k = - \sum_i j_i \nabla \left(\frac{\mu_i}{T} \right) + \sum_p w_p \frac{A}{T} \quad (14)$$

where j_i and w_p describe flows and reaction rates, respectively, and $\nabla(\mu_i/T)$ and A/T the generalized forces F_k , concentration or density gradients and chemical affinities, which measure the deviation from chemical equilibrium. Equation 14 clearly shows the two possibilities to explain the hysteresis (two different entropy production rates differing by a factor of 2–3 at otherwise identical solar intensity conditions). The first term involves a change in transport properties, the second a change in chemical (interfacial) rate (rate of evaporation).

A switch to a slower diffusion transport mode of water supply (first term in eq 14) at low solar intensity (eclipse) is not supportable by experimental evidence, since a similar eclipse-induced hysteresis is observed for the tree base and for an elevation of 11 m on the tree trunk below the crown (Figure 7). It also contradicts the observed fast response within the tensile strength water, observed with infrared images, which suggests a fast coupling of evaporation with sap transport in the trunk (Figure 9). If a transport problem occurs, which means stored or depleted water would be critically involved, then the sap flow decrease should also not exactly coincide with the decrease in solar intensity during the eclipse (Figure 7). If stored water would have been depleted, then the sap flow should have decreased slower than the solar light intensity during the eclipse. This was not observed. But there was interestingly a clear delay of 15–20 min in the renewed increase in sap flow during the recovery period of eclipse-mediated solar irradiation. For the above-mentioned reason of a still 5–10% solar light intensity, also a closure of leaf stomata can be excluded. Stomata are too sensitive for light, and even during the full eclipse around Munich stomata closure in leaves could be excluded.²² Furthermore, the hysteresis was observed for different tree species, which were not under stress conditions.

Therefore, only the second term in eq 14 may be responsible for the bistable steady-state evaporation observed (Figures 7 and 8), calculable from eq 10 and yielding the steady-state situation depicted in Figure 4. This means that an intrinsic kinetic reason is responsible for the bistable evaporation mechanism observed. The rate constant w_p in eq 14, corresponding to k_3 in eq 9a, will gradually increase and will then assume two states as derivable for eq 11 and expressed in Figure 4. When the entropy production σ described in eq 14 is multiplied with the temperature T , the energy turnover σT is obtained. Two states of energy turnover during tensile water evaporation are thus to be expected. The measured evaporation hysteresis reflects the transition between the two states $Q'P'$ and PQ in Figure 4 during the eclipse.

Such a bistable mechanism for water evaporation has been obtained by considering reasonable tensile water kinetics, including hydrogen-bond dynamics, which turned out to be compatible and related with a generalized VdW equation, which considers the intermolecular forces between water molecules and between water and the surface of the water conduits only. The state transition (Figure 4) of tensile strength water in the mesoscopic environment of tree leaves must thus involve autocatalytic mechanisms leading to self-organization as explained by the van der Waals eq 7 or by the equivalent kinetic autocatalytic eq 12 (Brusselator-type autocatalytic reaction, described by Nicolis and Prigogine²⁰). This means that tensile water is able to self-organize via the feedback mechanisms, considering intermolecular bonding involved in the empirical and realistic van der Waals equation.

Besides, autocatalysis drives the system away from equilibrium, increasing the chemical affinity A (in eq 14) by increasing the ratio a/p or k_3/k_2 . A kinetically significantly more efficient

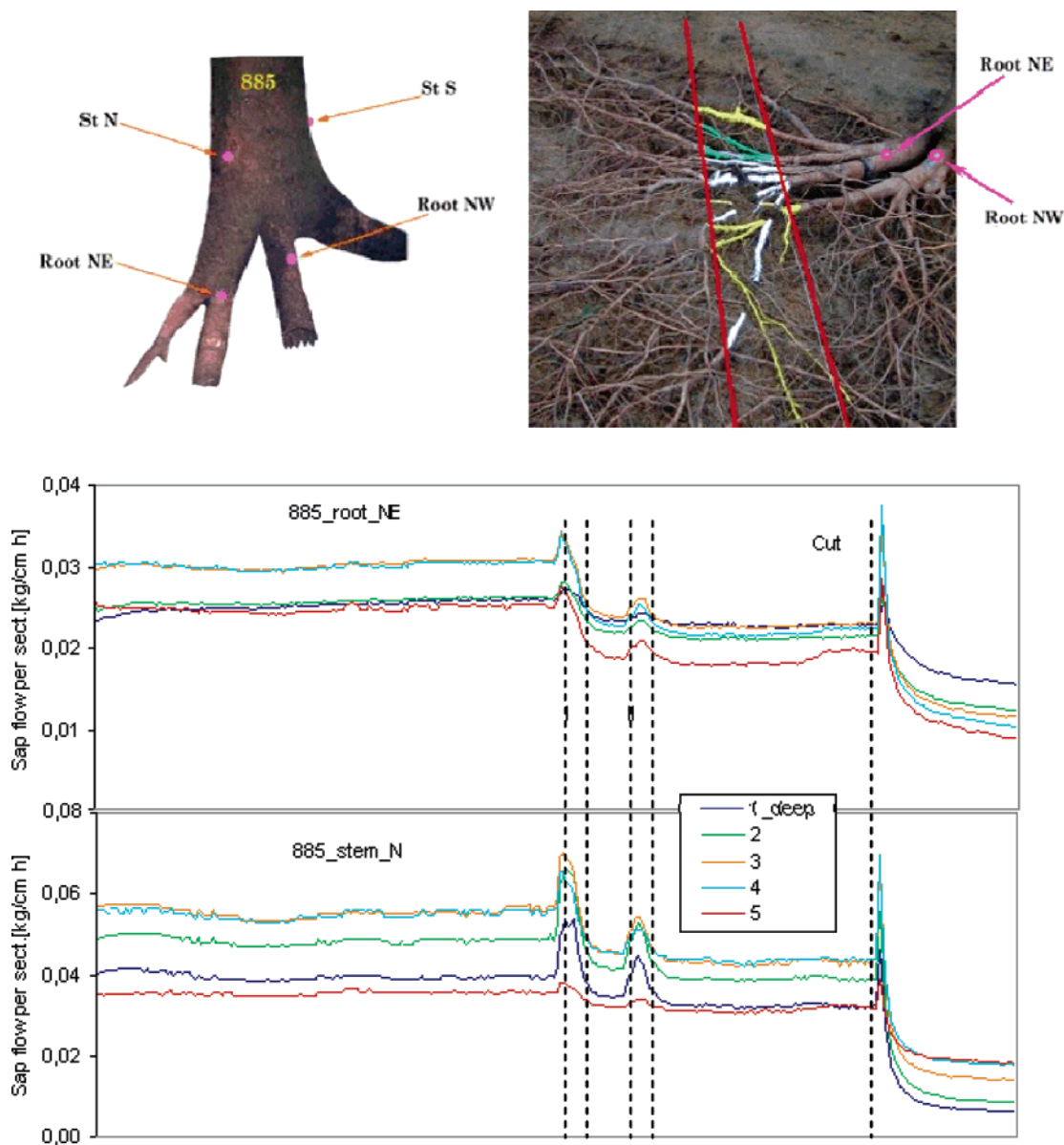


Figure 10. Detail view of the treated roots of a spruce and positions of sap flow sensors. Sensors were located on the opposite sides (south and north) of the stem and on two coarse roots (northeast and northwest). After the loading experiment was finished, the root system was opened by air stream, and the roots that were under loading were painted with different colors according to their relation to the concrete-measured coarse root. Roots painted with yellow, green, and white (from the left) were connected to the northeast root and roots painted yellow (from the right) were connected with the northwest root sensor. The sensor on the northeast root was installed on its branch, painted white.

evaporation of water is possible, as compared with equilibrium, which may have triggered evolution in the direction of tensile water technology. Trees are apparently taking advantage of a nonlinear, bistable mechanism (with an unstable state between) of evaporation and, under energy input, may switch from a less efficient mechanism to one with a higher evaporation rate (at sufficient solar intensity), taking advantage of an intrinsic excitability depending on internal parameters and external perturbation. Solar energy is obviously involved in adjusting the parameters that facilitate this transition. During the solar eclipse, which forced the trees to change from the more efficient to the less efficient rate, they lost that way a significant fraction of their evaporative power. This happened because within the parenchyma of illuminated leaves an internal temperature gradient is created that is intimately nonlinear feedback coupled with the buildup of tensile strength, the adjustment of intermolecular forces, and the generation of the water potential difference for evaporation, in relation to the temperature difference created by solar irradiation.

If our considerations are correct and eqs 9–12 indeed control water evaporation from leaves via a nonlinear bistable state (with an unstable state between), then more consequences for tensile water can be derived in a straightforward way. The kinetic Brusselator-type relation (eqs 9 and 9a), which followed from our kinetic model and is compatible and related with the van der Waals eq 5, can be shown to also sustain oscillations.²⁰ Oscillating mechanisms of this type have been shown to be attributable to soft materials.²⁶ In the same way, they can be applicable to water under tensile strength, which via hydrogen bonding and van der Waals forces can also be considered to be a soft material with a changeable form. A differential equation, considering the changeability of the form at each position u , describing damped oscillations can be derived. It has the structure

$$m \frac{d^2 V_u}{dt^2} + 2m\gamma_u \frac{dV_u}{dt} + k_u V_u = 0 \quad (15)$$

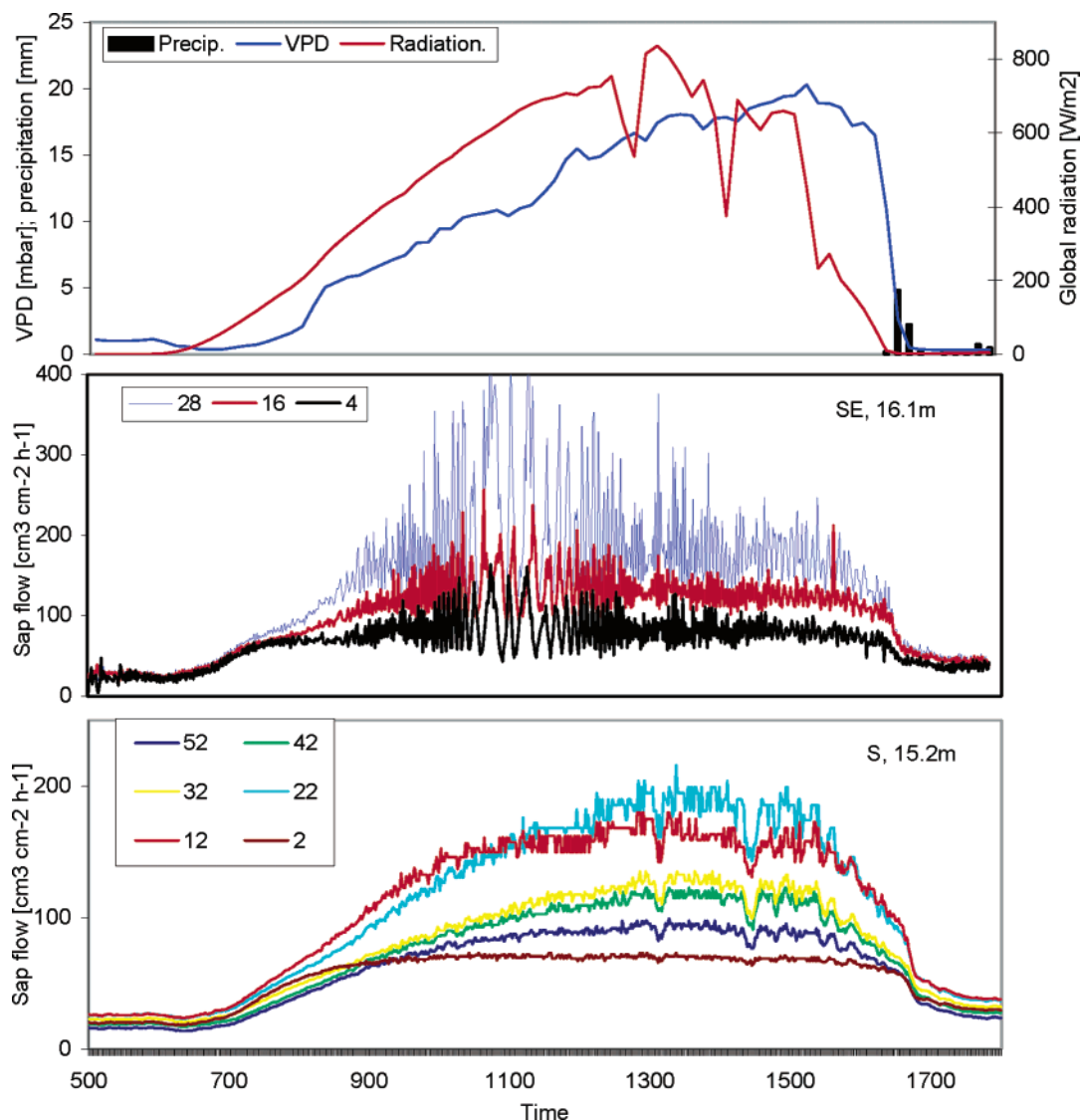


Figure 11. Diurnal courses of sap flow measured at different heights on different branches of a lime tree. Clear oscillations are observed in the presence of a stationary solar energy input. Top graphs: solar radiation, vapor pressure deficit, and precipitation monitored over the hours of 1 day. Middle graphs: sap flow oscillations measured at a height of 16.1 m in a southeast orientation with differently placed sensors. Bottom graphs: similar measurements at a height of 15.2 m in south direction for different depths.

where V expresses the molar volume, with the elastic coefficient k_u and the damping coefficient γ_u , which depend on the position u .

Since, as explained above, the intermolecular forces of the van der Waals equation will include the molecular interactions between water molecules and the elastic walls of the water conduits, the soft material oscillations explained by eq 15 will thus reflect the soft matter oscillations of the tensile water–conduit system. Such predicted oscillations can be observed in reality in trees. Auto-oscillating xylem sap flow is actually observed in plants such as sunflower or wheat, either spontaneously or influenced by external factors (e.g., watering).¹² Similar oscillations have also been observed in roots, stems, and branches of trees. Oscillations in a stem were only seen in the case of big trees with a big crown in open or partially open space. Sometimes, during a sunny day, a tree may show significant oscillations in the sap transport behavior, as demonstrated in Figure 11 with a lime tree in Sobesice. It is seen that sap oscillations may occur even though solar irradiation and the vapor pressure deficit are reasonably stable. The amplitudes for sap oscillations clearly change with solar intensity and are different for sunny and cloudy periods, as to be expected

since the solar energy input will control the energetics and oscillation dynamics of the system. A preliminary frequency analysis (Fourier transformation) for the special case of the lime tree studied in Figure 11 shows that for a narrow time window with approximately stable external conditions, e.g., for 20 min at 12.00 a.m. in Figure 11, a clear single frequency of 0.22 cycles per minute is found (period of 4.54 min). If however a large time window of 8 h is selected, then several oscillations are found with decreasing amplitudes between 0 and 0.3 cycles per minute.

According to the theory of nonlinear systems, a transition from a steady state to an oscillating system may simply arise due to changes in the parameter constellation. Small parameter changes may be the reason for a transition into the oscillating state. Also, when sap flow in trees is interrupted by severing a large branch, the cut sap water column may retract toward oscillations. But in reality only a change of direction in sap flow is observed with a subsequent relaxation to zero flow. In this case, we may observe a strongly damped relaxation phenomenon. All together it may be concluded that oscillations in tensile strength water systems are real. They have up to now been explained phenomenologically, assuming complicated

biological feedback mechanisms between root resistance and stomata aperture dynamics.¹² But it turns out here that the tensile water–conduit system itself can oscillate due to the nonlinear intermolecular and molecular–conduit wall interactions involved. Further experiments will be needed to deepen our understanding of these phenomena.

There is another phenomenon that can directly be derived from the Brusselator-type kinetics eqs 9–12 or its equivalent, the nonlinear van der Waals equation. It has the possibility to initiate catastrophic events. Very small perturbations can induce catastrophic changes. Mathematical analysis identifies the phenomenon as a Riemann–Hugoniot catastrophe.²⁰ A cubic equation of the type

$$4u^3 + 27z^2 = 0 \quad (16)$$

results with $u = u(A, B, k_{1-4})$ and $z = z(A, B, k_{1-4})$, functions depending on the kinetic factors from the Brusselator-type eqs 9 and 9a or, equivalent, on thermodynamic parameters, p , a , and b , from the VdW eq 5. It describes a “conflict” curve, which separates the parameter area with a bistable (Figure 4) solution from a parameter area with a single solution. Basically, this means that depending on the pressure, which can become negative to act as tensile strength, and on the intermolecular forces between water molecules, which can be disturbed by pollutants dissolved, the tensile strength may collapse. The tensile strength water may shift out of the bistable phase region to the neighboring phase region with only one steady-state behavior. This mathematical situation, which may also be triggered by small parameter changes, obviously describes the catastrophic phenomenon of cavitation, which is well-known to occur in trees. It is the spontaneous rupture of water columns under tensile strength, which can be acoustically detected with a microphone. The highly critical physical chemistry of this phenomenon, together with the very special evaporation process of tensile water molecules (eqs 9a and 11) have been made responsible for part of pollution-mediated forest decline.¹⁹

Since the oscillations as well as catastrophic all-or-none rupture of tensile water can be directly derived from the Brusselator-type and the corresponding van der Waals equation and are real, the hysteresis derived for solar evaporation in leaves from the same van der Waals equation should be equally real. In this case, we are indeed dealing with a special bistable mechanism of the evaporation of tensile strength water from plants. As the S-shape evaporation curve with the two-state character of evaporation (eq 11) (Figure 4) suggests and Figures 6–8 confirm, the evaporation of tensile strength water is thermodynamically different from the evaporation of ordinary water. This can, by the way, already be seen from the Clausius–Clapeyron equation, which describes the heat of evaporation L even though the use of this equation from reversible thermodynamics may lead to an apparent contradiction

$$L = T \frac{dp}{dT} (V_1 - V_2) \quad (17)$$

where dp/dT is the temperature gradient of the vapor pressure and $(V_1 - V_2)$ is the difference in molar volumes in the vapor and liquid state, respectively. Tensile strength (stretched) water has a molar volume, which is clearly larger than the molar volume of ordinary water (Figure 2). The heat of evaporation should therefore be smaller for evaporation of tensile strength water compared to ordinary water ($L_{\text{tensile water}} < L_{\text{water}}$). In principle, a difference may be understandable, because there is already energy stored in the tensile state of water pulled up into

the leaves. But low-density water, such as cold or supercooled water, or ice has a higher heat of evaporation because the water molecules are held more firmly and more hydrogen bonds are active. This should also be the case for tensile water, which is in a low-density state and held together by stronger intermolecular bonds than ordinary water. It is known that $2261 + 335$ kJ of energy per kilogram of water is released to convert water vapor first to water and then into ice with an expanded but stronger bonding structure. These energy quantities are additionally needed and absorbed when ice is reconverted into water and water vapor. Similar to the more energy-demanding evaporation process of ice, one can imagine that more energy is needed to evaporate water from the tensile state. While energy is released during conversion of water into ice or an ice-like state, about 2–3 times this energy has technically to be invested into a cooling process to achieve the necessary entropy reduction and heat extraction. In total, energy has therefore to be provided to produce the ice-like tensile state. In the trees, ultimately solar energy is activated to put water into an icelike but less ordered state of expansion, which mobilizes additional hydrogen bonds. This occurs, as discussed, via an irreversible process. The Clausius–Clapeyron equation has therefore to be completed by considering additional irreversible entropy turnover $\Delta S_{\text{irr}} = Q_{\text{irr}}/T$. This leads to an increased heat of evaporation $L_{\text{irr}} \rightarrow L + Q_{\text{irr}}$, replacing eq 17. This resolves the contradiction found with eq 17 and suggests the following interpretation: Nature, with its tensile state water technology, has apparently exploited the fact that expanded water structures (similar to ice or supercooled water) in nano- and microstructured environments require more heat of evaporation. The energy difference, to the heat of evaporation of normal water, is thus in principle made available to the tree, where it is utilized to induce negative pressure and to perform mechanical work.

We can now return to eq 3 for water evaporation E and introduce the above-discussed nonlinearity, which arises because of molecular (hydrogen bond and van der Waals) interactions between water species and between water and the cellulose conduit walls via the van der Waals eq 5 and the resulting nonlinear behavior of the molar water volume $V \rightarrow V_{\text{nonlinear}} \rightarrow V_n$. The water potential gradient $\Delta\Psi$, which controls evaporation via the molar water volume V (activity or concentration of water) along the volume axis of the p – V diagram of Figure 2, of course depends on the molar water volume, which is obtained by solving the cubic eq 7 or 12. In this way, returning to the simple eq 3, since the molar volume is bistable, evaporation will also become a bistable process

$$E = \frac{Q}{cc_p} \frac{d\Psi}{dT} = \frac{Q}{cc_p} \frac{d\Psi}{dV_n} \frac{dV_n}{dT} = k_3 V' \quad (18)$$

In this equation, it was considered that eq 3 for the evaporation (E) can be identified with the derived kinetic eq 11 for the evaporation process. It follows from eq 18 that the temperature gradient $d\Psi/dT$ is the dominant nonlinear function for evaporation. A relation for this temperature gradient of the water potential ψ can now be derived

$$\frac{d\Psi}{dT} = \frac{cc_p k_3}{Q} V' \quad (19)$$

It is indeed a nonlinear function, as Figure 4 shows for the S-shaped behavior of V or V' , which enters into eq 18, and as initially postulated for the dynamics of tensile water evaporation. For a given solar heat input Q , two different rates of evaporation E (eq 18 and Figure 4 with $a/p = k_3/k_2$ and $V = V'$),

corresponding to two different temperature gradients of the water potential $d\Psi/dT$ (eq 19), are possible. One gradient is for ordinary water and the other for the expanded, tensile water with the increased concentration of active hydrogen bonds. These two gradients explain the hysteresis in sap evaporation observed during the solar eclipse, and they also explain why nature was able to evolve a solar energy technology based on the energy of evaporation pulling tensile water. In fact, a more difficult to evaporate tensile water phase is produced that absorbs more solar energy for evaporation, and the free energy difference to that of ordinary water is used to do mechanical or desalination work. Artificial systems will have to provide analogous conditions.

Evaporation will thus, depending on external conditions, follow the nonlinear (tensile-strength-producing, bistable, oscillating, or chaotic) properties of eq 12 discussed in this manuscript, which is compatible with and related to the VdW equation. This is expected to occur in a morphologically self-organizing process. Solar energy, by evaporation of water molecules from suitable evaporation structures (leaf parenchyma), is gradually changing the bonding structure of water, by increasing the ratio of reaction rates k_3/k_2 (or a/b , as shown by eq 13b) and pushing it off equilibrium into a bistable state. It would explain why evaporation could change 2–3 times while the ambient temperature stays constant within 1–2 °C. Critical for evaporation is then obviously the temperature gradient of the water potential (in eq 18) in the leaf parenchyma, which will be controlled by the nonlinear intermolecular forces between water molecules (which is the origin of its van der Waals and Brusselator-type kinetic behavior) and builds up during solar illumination. During evolution, the structural–molecular environment in plant tissues will have been adjusted to maximize evaporation and coupled water transport. In contrast to earlier interpretations,¹² nonlinear behavior of sap movement in trees can already be explained on the basis of intermolecular forces between water molecules as expressed via the van der Waals/Brusselator equation (but nonlinear biological mechanisms may be superposed). Water molecules within a suitable mesoscopic tree environment are obviously statistically behaving as “microcanonical” systems, which are not in equilibrium. The difficulty in defining phase transitions in small molecular clusters is well-known and still provides a challenge. Here, the transition from small water clusters, linked by hydrogen bonds, to larger hydrogen-bond-controlled aggregates and structures, which fill and are stabilized by capillary spaces, will be in the center of interest. Exploitation of microcanonical properties of water with expanded stronger interlinked structure in adapted mesoscopic structures has apparently directly guided evolution of water conduits toward efficient water transport and (leaf) evaporation properties. The mesoscopic structure of the tree water conduit systems apparently determines the boundary of the microcanonical ensembles by optimizing hydrophilic conditions, which are aiding in suppressing cavitation.

This nonlinear coupling of evaporation to tensile strength water is considered to be the key to efficient evaporative solar energy conversion in trees. It is proposed as a model system to better describe both the energetics and the dynamics of sap behavior and sap movement in trees. It should motivate a new look at plant water physiology on the leaf level. The very successful concept of water potential of plant physiology, for example, derived from reversible thermodynamics, appears to be a simplified concept only. Nature has apparently optimized structure and function of water conduits and water evaporation leaf morphology around the nonlinear physical chemistry of

water intermolecular forces. It has optimized the system via adapted water conduit structures toward an energy-converting vapor machine based on irreversible thermodynamics.

Consequences for Understanding Tensile-Water-Based Technology. At present, in physical chemical teaching, the van der Waals equation is essentially used to indicate the possible transition to instability (e.g., superheated water, under cooled vapor), while the Maxwell shortcut at ambient pressure is used to force the van der Waals properties back into the scheme of reversible thermodynamics. This is possible because the Maxwell criterion applied for the shortcut fixes the adopted entropy values of the system as properties of state. Carnot cycles for energy conversion by vapor machines, as we know them, can thus be properly described. We have here derived a kinetic mechanism for tensile water behavior, which is entirely compatible and related with the VdW behavior and suggests that it describes a realistic physical chemical situation. We may say that, if we allow the entropy to be a quantity of state (independent of the process pathways), then we can operate vapor machines subject to reversible thermodynamics. If, however, we do not allow this, by providing a mesoscopic environment so that water can react as microcanonical ensembles, then the system may, under solar energy input, follow the laws of irreversible thermodynamics, shifting away from equilibrium. This way it is permitting new states including self-organization, bistability, chaos, and oscillations, which directly follow from the derived tensile water kinetics. Nature, during evolution, has discovered this possibility and developed a far from equilibrium vapor machine, which is functioning in trees. For this purpose, it had to develop sophisticated structural conditions. They include water conduits, which suppress cavitation, and a leaf parenchyma morphology, which allows the transition of water molecules into the gas phase from an increased molar volume state, which, similar to ice, allows a high degree of hydrogen-bond-mediated water cohesion. The aim of future efforts should be to understand the irreversible thermodynamic nature and the kinetics of tensile water in detail to follow the example of nature toward tensile water technologies, powered by solar energy.

References and Notes

- (1) Zimmermann, M. H. In *Wood Science*; Springer-Verlag: Berlin, Germany, 1983; p 144.
- (2) Larcher, W. *Physiological Plant Ecology*; Springer-Verlag: Berlin, Germany, 1995.
- (3) Nobel, P. S. In *Physicochemical and Environmental Plant Physiology*; Academic Press: Heidelberg, Germany, 1991.
- (4) (a) Boehm, J. *Ber. Dtsch. Bot. Ges.* **1889**, 46–56. (b) Boehm, J. *Ber. Dtsch. Bot. Ges.* **1893**, 203.
- (5) Dixon, H. H. *Transpiration and the Ascent of Sap in Plants*; McMillan: London, 1914.
- (6) Huber, B. In *Die Saftströme der Pflanzen*; Springer-Verlag: Berlin, Heidelberg, Germany, 1956.
- (7) Scholander, P. F.; Hammel, H. T.; Bradstreet, E. D.; Hemmingsen, E. A. *Science* **1965**, 148, 339.
- (8) Kramer, P. J. *Water Relations in Plants*; Academic Press: New York, 1983.
- (9) Boyer, J. S. *Annu. Rev. Plant Physiol.* **1985**, 36, 473.
- (10) Hayward, T. J. *Am. Sci.* **1971**, 95, 434.
- (11) Briggs, L. J. *J. Appl. Physiol.* **1950**, 21, 721.
- (12) Meleshchenko, S. N. *Russ. J. Plant Physiol.* **2000**, 47, 826.
- (13) Nadezhdina, N.; Cermák, J.; Nadezhdin, V. In *Proceedings of the 4th International Workshop*, Zidlochovice, Czech Republic, Ěermák, J., Nadezhdina N., Eds.; IUFRO Publications, Publishing House of Mendel University: Brno, Czech Republic, 1998; p 72.
- (14) Nadezhdina, N.; Cermák, J.; Ceulemans R. *Tree Physiol.* **2002**, 22, 907.
- (15) (a) Nadezhdina, N.; Cermák, J.; The Technique and Instrumentation for Estimation of the Sap Flow Rate in Plants. Patent No. 286438 (PV-1587-98), 2000 (in Czech). (b) Nadezhdina, N.; Cermák, J. In *The Supporting Roots of Trees and Woody Plants: Form, Function, and*

Physiology; Stokes, A., Ed.; Developments in Plant and Soil Sciences 87; Kluwer Academic Publishers: Boston, MA, 2000; p 227. (c) Nadezhdina, N., Eermák, J. In *Spruce Monocultures in Central Europe: Problems and Prospects*; Klimo, E., Hager, H., Kulhavy, J., Eds.; EFI Proceedings 33; European Forest Institute: Joensuu, Finland, 2000; p 167.

(16) Cermak, J., Jenik, J., Kucera, J., Zidek, V. *Oecologia* **1984**, *64*, 145.

(17) Ladefoged, K. *Physiol. Plant.* **1963**, *16*, 378.

(18) Haken, H. *Synergetics: An Introduction*; Springer: Berlin, Germany, 1983.

(19) Tributsch, H. *J. Theor. Biol.* **1992**, *156*, 235.

(20) Nicolis, G., Prigogine, I. In *Self-Organization in Nonequilibrium Systems*; John Wiley: New York, 1977; p 173.

(21) Eisinger, W.; Schwartz, T. E.; Bogomolni, R. A.; Taiz, L. *Plant Physiol.* **2000**, *122*, 99.

(22) Häberle, K.-H.; Reiter, I.; Patzner, K.; Heyne, C.; Matyssek, R. *Meteorol. Z.* **2001**, *10*, 201.

(23) Nadezhdina, N.; Cermák, J.; Tributsch, H. In *Proceedings of the 5th International Workshop "Plant Water Relations and Sap Flux Measurements"*, Firenze, Italy, Nov 9–10, 2000; Tognetti, R., Raschi, A., Eds.; 2000; p 155.

(24) Nadezhdina, N.; Tributsch, H.; Cermak, J. *Ann. For. Sci.*, in press.

(25) Nadezhdina, N.; Cermak, J.; Nadezhdina, V.; Gasperek, J.; Ulrich, R.; Neruda, J. *Eur. J. For. Res.*, submitted for publication.

(26) Morikawa, Y., Yamaguchi T., Amemiya, T. *Forma* **2000**, *15*, 249.